

03,09

Peculiarities of the behavior of the temperature dependence of high-frequency conductivity of disordered semiconductors in the terahertz frequency range

© M.A. Ormont, A.A. Lyashenko

Department of Physics, Moscow State University,
Moscow, Russia

E-mail: ormont.73@mail.ru

Received October 11, 2024

Revised November 18, 2024

Accepted November 19, 2024

The analysis of the features of electron hopping transport in the impurity band of a disordered semiconductor with hydrogen-like impurities, associated with the behavior of the temperature dependence of high-frequency conductivity in the low-temperature region, is carried out. Based on the pair approximation, the numerical calculation of the temperature dependence of the real part of the high-frequency conductivity of a disordered semiconductor in the terahertz frequency range was performed, in which the transition from an almost linear to a quadratic frequency dependence of the real part of the conductivity was observed under low-temperature conditions with increasing frequency. It is shown that taking into account the Coulomb interaction between electrons in pairs causes a non-monotonic saturation of the temperature dependence of high-frequency conductivity with decreasing temperature due to the opposite direction of changes in the relaxation and resonance contributions to conductivity with changing temperature. The increase in phononless conductivity with decreasing temperature is due to the main role of the Coulomb interaction between electrons in resonant pairs at low temperatures, $e^2/kr_\omega > \hbar\omega$ (r_ω — optimal hopping distance at frequency ω).

Keywords: high-frequency hopping conductivity, deviations from the universality of the frequency dependence of conductivity, disordered semiconductors.

DOI: 10.61011/PSS.2025.01.60574.2-25

1. Introduction

Obtaining information about the features of hopping transfer mechanisms in disordered semiconductors is complicated by the universality of the power-law frequency dependence of conductivity, $\sigma(\omega) \sim \omega^s$ (s — constant; as a rule, $0.5 < s < 1$), that well describes $\sigma(\omega) = \sigma_1(\omega) + i\sigma_2(\omega)$ of disordered semiconductors in a wide frequency range. Studies of the temperature dependence of AC conductivity play an important role for this reason [1]; in particular, in the frequency range, in which deviations of the frequency dependence of the conductivity of disordered semiconductors from universality ($s \approx 1$) are observed.

The high-frequency conductivity of disordered semiconductors with hydrogen-like impurities is usually described using the concept of a frequency-dependent optimal hopping distance r_ω , which significantly exceeds the radius of localization of states a and decreases with the increase of frequency. Nonmonotonic frequency dependences given by the theory for resonant (phononless) and relaxation (phonon) contributions to conductivity [2–6]

$$\begin{aligned}\sigma_1^{res}(\omega) &\sim r_\omega^n \omega^m \sim \omega^m \ln^n(\omega_c/\omega), \\ \sigma_1^{rel}(\omega) &\sim \tilde{r}_\omega^l \omega^q \sim \omega^q \ln^l(\omega_{ph}/\omega),\end{aligned}\quad (1)$$

can be approximated by the power law $C\omega^s$ with exponent $s(\omega)$ decreasing with the increase of frequency [7]; here σ_1^{res} , σ_1^{rel} — the real parts of phononless and relaxation contributions to conductivity, $\sigma_1(\omega) = \sigma_1^{res}(\omega) + \sigma_1^{rel}(\omega)$, n, m, l, q — integers, ω_c — the frequency at which the optimal hopping distance r_ω for resonant conductivity becomes of the order of the radius of localization of states, ω_{ph} — the characteristic phonon frequency, which is the frequency of electron transition attempts during relaxation conductivity.

However, the frequency dependences of the conductivity of the form (1) with the values of the parameter $A = e^2/\kappa a \hbar \omega_c \approx 1/2$ (where κ — the dielectric constant of the medium, $\omega_c = 2I_0/\hbar$; $I_0 \approx e^2/\kappa a$ — the preexponential factor of the resonance integral) which are typical for shallow impurities do not describe the transition of the frequency dependence of the real part of the low-temperature conductivity $\sigma_1(\omega)$ from almost linear to quadratic with the increase of frequency that is observed in SiP [8–10], SiB [11]. At high frequencies, phononless conductivity prevails over relaxation conductivity; however, the Coulomb interaction between electrons in resonant pairs plays a main role, $\hbar\omega < e^2/\kappa r_\omega$, in a wide frequency range, $\omega < \omega_c$, according to the theory and the frequency dependence of phononless conductivity $\sigma_1^{res}(\omega)$ remains close to linear ($s \approx 1$) up to the frequency $\omega_m \approx 0.07\omega_c$

corresponding to the maximum $\sigma_1^{res}(\omega)$ [12]. It should be noted that the frequency dependence of conductivity will be nonmonotonic because the frequency dependence of the optimal hopping distance; in the paired approximation for phononless conductivity, the frequency dependence of the optimal hopping distance r_ω is related to the hybridization of wave functions of an isolated pair of centers and is determined by the equation $\hbar\omega = 2I_{\lambda\lambda'}(r_\omega)$, where $I_{\lambda\lambda'} = I_0 \exp(-r_{\lambda\lambda'}/a)$ — resonance integral, $r_{\lambda\lambda'}$ — center-to-center distance, λ — center number.

A significantly smoother transition than is observed experimentally from the sublinear (relaxation, phononless) to the subquadratic (phononless) frequency dependence of the conductivity $\sigma_1(\omega)$ in the mode with a variable hopping distance can be explained only at small values of the parameter $A < 10^{-5}$, which are atypical for shallow impurities. The dependence of the conductivity $\sigma_1(\omega)$ will be nonmonotonic with a maximum in the vicinity of the transition frequency [12]. However, the non-monotonicity of the frequency dependence of the conductivity $\sigma_1(\omega)$ of disordered semiconductors in the transition frequency range predicted by the theory has not been experimentally detected [8–11].

The calculation of the real part of low-temperature conductivity ($e^2/\kappa r_\omega$, $\hbar\omega > kT$) in a pair approximation made in Ref. [13] showed that the transition from an almost linear to a quadratic frequency dependence $\sigma_1(\omega)$ can be associated with the transition from conductivity with variable hopping distance r_ω to conductivity with constant hopping distance r_{opt} with the frequency increase. The transition from a variable hopping distance $r_\omega = a \ln(\omega_c/\omega)$ to a constant hopping distance $r_{opt} \approx 4a$ occurs at $r_{opt} \approx r_\omega$ ($\omega_{opt} \approx 0.02\omega_c$) in case of a phononless conductivity; $\omega_c/2\pi \sim 10^{13}$ Hz for Si:P. The phononless conductivity has the following known form [3,6] at low frequencies $\omega < \omega_{opt}$ ($r_\omega > r_{opt}$) in the variable hopping distance mode

$$\sigma_1^{res}(\omega) = (\pi^2/3)e^2 a \rho_0^2 r_\omega^4 \omega (\hbar\omega + e^2/\kappa r_\omega); \quad (2)$$

ρ_0 is the density of states, considered constant. Since the Coulomb interaction between electrons inside resonant pairs of centers plays the main role [12], $\hbar\omega < e^2/\kappa r_\omega$, the frequency dependence of phononless conductivity remains sublinear ($s \approx 0.8$)

$$\sigma_1^{res}(\omega) = (\pi^2/3)e^4 a \rho_0^2 r_\omega^3 \omega / \kappa. \quad (3)$$

The main contribution to conductivity is made by electronic transitions within pairs with a center-to-center distance of the order of r_{opt} at high frequencies $\omega > \omega_{opt}$ ($r_{opt} > r_\omega$) according to Ref. [13], when the effects of hybridization are insignificant. At high frequencies in the constant hopping distance mode r_{opt} , the phononless conductivity is equal to

$$\sigma_1^{res}(\omega) = (\pi^2 C_1/3)e^2 \rho_0^2 a^5 \omega (\hbar\omega + e^2/\kappa r_{opt}), \quad (4)$$

where $C_1 = 315$ is the numerical coefficient. The frequency $\omega_{opt} \approx 0.02\omega_c$ ($r_\omega \approx r_{opt}$) at which the transition to a constant hopping distance occurs, of the order of the crossover frequency in (4), $\hbar\omega_{cr} \approx e^2/\kappa r_{opt}$ ($\omega_{cr} \approx 0.1\omega_c$); i.e., the transition from linear to quadratic frequency dependence of the real part of the conductivity occurs in the vicinity of the frequency $\omega_{opt} \sim \omega_{cr}$ [13]. We have the following equation under conditions of low temperatures in the high frequency range, when the Coulomb interaction between electrons in pairs with an optimal center-to-center distance r_{opt} can be neglected, for phononless conductivity

$$\sigma_1^{res}(\omega) = (\pi^2 C_1/3)e^2 \rho_0^2 a^5 \hbar\omega^2. \quad (5)$$

The phononless conductivity transitions to a constant hopping distance under conditions $kT > \hbar\omega$, $e^2/\kappa r_{opt}$ in the high frequency range like in the case of low temperatures. The transition for phononless conductivity from a variable r_ω to a constant hopping distance r_{opt} occurs at $r_{opt} \approx r_\omega$ ($\omega_{opt} \approx 0.02\omega_c$) according to Ref. [14]. The phononless conductivity at low frequencies $\omega < \omega_{opt}$ ($r_\omega > r_{opt}$) in the variable hopping distance mode r_ω is equal to [7]

$$\sigma_1^{res}(\omega) = (\pi^2/3)e^2 a \rho_0^2 \hbar r_\omega^4 \omega^2, \quad (6)$$

i.e. $\sigma_1^{res}(\omega)$ (6) has a subquadratic character ($s \approx 1.5$).

The phononless conductivity has the form (5) at high frequencies $\omega > \omega_{opt}$ ($r_{opt} > r_\omega$), when the effects of hybridization are insignificant, in the mode with a constant hopping distance r_{opt} . High-frequency phononless conductivity is independent of temperature according to (6), (5) under conditions $kT > \hbar\omega$, $e^2/\kappa r_{opt}$. The frequency of transition of phononless conductivity from a variable to a constant hopping distance is of the order of the crossover frequency, in the vicinity of which the transition from relaxation conductivity to phononless conductivity occurs [14]. Accordingly, the transition from the sublinear ($s < 1$) to the quadratic frequency dependence $\sigma_1(\omega)$ with the increase of the temperature can persist and be caused by the transition from relaxation conductivity with variable hopping distance to phononless conductivity with constant hopping distance with the increase of the frequency.

We would like to remind that the expression for the real part of the high-frequency relaxation conductivity has the following form in the low temperature range, $e^2/\kappa \tilde{r}_\omega > kT$ [5]

$$\sigma_1^{rel}(\omega) = \pi^2 e^4 \rho_0^2 a \tilde{r}_\omega^3 \omega / (6\kappa), \quad (7)$$

where $\tilde{r}_\omega = (a/2) \ln(\omega_{ph}/\omega)$ is the optimal hopping distance for relaxation conductivity at the frequency ω ; $\omega_{ph}/2\pi \sim 10^{13}$ Hz for Si:P. It should be noted that the expressions for the real parts of low-temperature relaxation conductivity (7) and low-temperature phononless conductivity in the transition frequency range (3) have a single form ($s \approx 0.8$); this, in particular, is associated with the difficulty

of interpreting experimental data on the frequency dependences of the conductivity of disordered semiconductors and obtaining information about the features of the mechanism of hopping charge carrier transfer in them.

The real part of the relaxation conductivity begins to depend on temperature as the temperature increases, $kT > e^2/\kappa\tilde{r}_\omega$; at the same time, its frequency dependence does not significantly change ($s \approx 0.6$) [4]

$$\sigma_1^{rel}(\omega) = \pi^4 e^2 \rho_0^2 a k T \tilde{r}_\omega^4 \omega / 24. \quad (8)$$

The interpolation expression for the real part of the relaxation conductivity has the form [7]

$$\sigma_1^{rel}(\omega) = (\pi^4 / 24) e^2 a \rho_0^2 \tilde{r}_\omega^4 (kT + (4/\pi^2) e^2 / \kappa \tilde{r}_\omega). \quad (9)$$

It should be noted that the expression (6) for phononless conductivity at high temperatures, $kT > \hbar\omega$, $e^2/\kappa r_\omega$, coincides with the expression for phononless conductivity in the high-frequency range at low temperatures, $\hbar\omega > e^2/\kappa r_\omega > kT$; the Coulomb interaction between electrons in resonant pairs can be neglected in these cases. However, the Coulomb interaction between electrons in resonant pairs plays a main role, $\hbar\omega < e^2/\kappa r_\omega$, in a wide frequency range at low temperatures, according to [12]; at the same time, the frequency dependence of the real part of low-temperature phononless conductivity (3), $e^2/\kappa r_\omega > \hbar\omega > kT$, turns out to be weaker than the frequency dependence of phononless conductivity at high temperatures (6), $kT > \hbar\omega$, $e^2/\kappa r_{op}$. The phononless conductivity of a disordered semiconductor increases with the decrease of the temperature at a constant frequency according to (2), (3), and (6), while the relaxation conductivity of (9), on the contrary, decreases. Accordingly, the temperature dependence of the conductivity $\sigma_1(\omega, T)$ in the low temperature range may have a nonmonotonic character, which is attributable to the prevalence of the phononless contribution to the conductivity in the transition frequency range and the main role of the Coulomb interaction between electrons in resonant pairs at low temperatures, $e^2/\kappa r_\omega > \hbar\omega > kT$.

The ratio of relaxation (7) and phononless (3) contributions to conductivity, $\sigma_1(\omega, T) = \sigma_1^{res}(\omega, T) + \sigma_1^{rel}(\omega, T)$, is equal to

$$\sigma_1^{rel}(\omega) / \sigma_1^{res}(\omega) = (1/16) (\ln(\omega_{ph}/\omega) / \ln(\omega_c/\omega))^3. \quad (10)$$

The resonant contribution to low-temperature conductivity prevails over relaxation contribution, $\sigma_1^{rel}(\omega) / \sigma_1^{res}(\omega) \ll 1$ in case $\omega_{ph} \sim \omega_c$ in the frequency range $\omega < 0.1\omega_c$; formally, the ratio of contributions to conductivity does not depend on frequency, $\sigma_1^{rel}(\omega) / \sigma_1^{res}(\omega) \approx 5 \cdot 10^{-2}$, with $\omega_{ph} = \omega_c$.

Thus, the real part of the conductivity $\sigma_1(\omega, T)$ (at a given frequency) should decrease with an increase of temperature at the initial stage; this is not consistent with the dependences $\sigma_1(\omega, T)$ obtained in Ref. [8] in experiments on Si:P, according to which the conductivity

of $\sigma_1(\omega, T)$ reaches saturation monotonously decreasing as the temperature decreases (to $T \approx 3$ K). This discrepancy, related to the behavior of the temperature dependence of the high-frequency conductivity of disordered semiconductors in the low-temperature region, may be significant in assessing the degree of impact of Coulomb effects on the frequency dependence of the low-temperature conductivity of disordered semiconductors and necessitates its further study. The purpose of this work was to calculate the temperature dependence of the high-frequency conductivity of disordered semiconductors in the transition frequency range and to study the features of its behavior at low temperatures.

Calculation of the temperature dependence of high-frequency conductivity in the transition frequency range

The expression for the real part of phononless conductivity has the following form in the pair approximation according to the theory of hopping transport (see, for example, [15])

$$\sigma_1^{res}(\omega) = \frac{\pi e^2 \omega}{V_0} \sum_{\substack{\{\lambda, \lambda'\} \\ \lambda \neq \lambda'}} \left| \langle \psi_{\lambda\lambda'}^- | (\mathbf{n}, \mathbf{r}) | \psi_{\lambda\lambda'}^+ \rangle \right|^2 \times (n_F(\varepsilon_{\lambda\lambda'}^-) - n_F(\varepsilon_{\lambda\lambda'}^+)) \delta(\varepsilon_{\lambda\lambda'}^- - \varepsilon_{\lambda\lambda'}^+ + \hbar\omega). \quad (11)$$

The electronic hopping transport through the impurity zone is determined by the ground impurity states in the transition frequency range (for Si:P $\nu \sim 10$ GHz – 1 THz) under low temperature conditions. The matrix elements in the considered case of hydrogen-like impurity centers are equal to [13]

$$\langle \psi_{\lambda\lambda'}^- | (\mathbf{n}, \mathbf{r}) | \psi_{\lambda\lambda'}^+ \rangle = (\mathbf{n}, \mathbf{r}_{\lambda\lambda'}) \frac{I_{\lambda\lambda'}}{\Gamma_{\lambda\lambda'}} + \frac{(\varepsilon_\lambda^0 - \varepsilon_{\lambda'}^0) \langle \psi_\lambda | (\mathbf{n}, \mathbf{r}) | \psi_{\lambda'} \rangle}{\Gamma_{\lambda\lambda'}}; \quad (12)$$

here $\psi_{\lambda\lambda'}^\pm = C_\lambda^\pm \psi_\lambda + C_{\lambda'}^\pm \psi_{\lambda'}$ — hybridized wave functions of the ground states of the electron $\psi_\lambda, \psi_{\lambda'}$ on isolated localization centers λ and λ' , \mathbf{n} — a unit vector parallel to external electric field, $\mathbf{r}_{\lambda\lambda'}$ — radius vector of the center λ' relative to the center λ , $n_F(\varepsilon)$ — average filling number of states with energy ε , V_0 — system volume, $\varepsilon_\lambda^0, \varepsilon_{\lambda'}^0$ — initial energies (excluding hybridization), $I_{\lambda\lambda'} = \langle \psi_\lambda | U_\lambda | \psi_{\lambda'} \rangle$ — resonance integral; $I_{\lambda\lambda'} = I_0 \exp(-r_{\lambda\lambda'}/a)$, $I_0 \approx e^2/\kappa a$, $\Gamma_{\lambda\lambda'} = \sqrt{(\varepsilon_\lambda^0 - \varepsilon_{\lambda'}^0)^2 + 4I_{\lambda\lambda'}^2}$. In the case of shallow impurity centers with weak doping, $a < N_d^{-1/3}$ (N_d — concentration of impurity centers), the potential energy of a localized electron at the location of the center with the number λ can be represented by in the form $U_\lambda = -e^2/\kappa|\mathbf{r} - \mathbf{r}_\lambda| + e\varphi(\mathbf{r}_\lambda)$;

here \mathbf{r}_λ — the radius vector of the center λ , $e\varphi(\mathbf{r}_\lambda)$ — the Coulomb shift caused by other charged centers at the point \mathbf{r}_λ .

The matrix elements in (12) have the following form for hydrogen-like impurities in the case of a large center-to-center distance, $r_{\lambda,\lambda'} > a$, in the approximation of the isotropic dispersion law [13]

$$\langle \psi_\lambda | (\mathbf{n}, \mathbf{r}) | \psi_{\lambda'} \rangle \approx \frac{r_{\lambda,\lambda'}^3}{a^2} \exp(-r_{\lambda,\lambda'}/a) \cos \theta, \quad (13)$$

where θ is the angle between the vectors \mathbf{n} and $\mathbf{r}_{\lambda,\lambda'}$, $\psi_\lambda(\mathbf{r}) = (1/\sqrt{\pi a^3}) \exp(-|\mathbf{r} - \mathbf{r}_\lambda|/a)$.

Proceeding from summation to integration in (11), for the real part of phononless conductivity we obtain [13,14]

$$\sigma_1^{res}(\omega) = \sigma_{1a}^{res}(\omega) + \sigma_{1b}^{res}(\omega) + \sigma_{1c}^{res}(\omega), \quad (14)$$

$$\begin{aligned} \sigma_{1a}^{res}(\omega) &= \frac{4\pi^2 e^2 \rho_0^2 \omega}{3} \\ &\times \int_{r_\omega}^{\infty} dr_{\lambda\lambda'} r_{\lambda\lambda'}^4 \int_{-\infty}^{\infty} d\varepsilon_{\lambda\lambda'}^- \int d\varepsilon_{\lambda\lambda'}^+ \Phi(\varepsilon_{\lambda\lambda'}^-, \varepsilon_{\lambda\lambda'}^+, r_{\lambda\lambda'}) \\ &\times \frac{I_{\lambda\lambda'}^2}{(\varepsilon_{\lambda\lambda'}^+ - \varepsilon_{\lambda\lambda'}^-)^2} (n_F(\varepsilon_{\lambda\lambda'}^-) - n_F(\varepsilon_{\lambda\lambda'}^+)) \delta(\varepsilon_{\lambda\lambda'}^- - \varepsilon_{\lambda\lambda'}^+ + \hbar\omega), \end{aligned} \quad (15.1)$$

$$\begin{aligned} \sigma_{1b}^{res}(\omega) &= \frac{4\pi^2 e^2 \rho_0^2 \omega}{3} \int_{r_\omega}^{\infty} dr_{\lambda\lambda'} \frac{r_{\lambda\lambda'}^6}{a^2} \exp(-r_{\lambda\lambda'}/a) \\ &\times \int_{-\infty}^{\infty} d\varepsilon_{\lambda\lambda'}^- \int d\varepsilon_{\lambda\lambda'}^+ \Phi(\varepsilon_{\lambda\lambda'}^-, \varepsilon_{\lambda\lambda'}^+, r_{\lambda\lambda'}) \frac{2I_{\lambda\lambda'}}{(\varepsilon_{\lambda\lambda'}^+ - \varepsilon_{\lambda\lambda'}^-)^2} \\ &\times \sqrt{(\varepsilon_{\lambda\lambda'}^+ - \varepsilon_{\lambda\lambda'}^-)^2 - 4I_{\lambda\lambda'}^2} (n_F(\varepsilon_{\lambda\lambda'}^-) - n_F(\varepsilon_{\lambda\lambda'}^+)) \\ &\times \delta(\varepsilon_{\lambda\lambda'}^- - \varepsilon_{\lambda\lambda'}^+ + \hbar\omega), \end{aligned} \quad (15.2)$$

$$\begin{aligned} \sigma_{1c}^{res}(\omega) &= \frac{4\pi^2 e^2 \rho_0^2 \omega}{3} \int_{r_\omega}^{\infty} dr_{\lambda\lambda'} \frac{r_{\lambda\lambda'}^8}{a^4} \exp(-2r_{\lambda\lambda'}/a) \\ &\times \int_{-\infty}^{\infty} d\varepsilon_{\lambda\lambda'}^- \int d\varepsilon_{\lambda\lambda'}^+ \Phi(\varepsilon_{\lambda\lambda'}^-, \varepsilon_{\lambda\lambda'}^+, r_{\lambda\lambda'}) \\ &\times \frac{((\varepsilon_{\lambda\lambda'}^+ - \varepsilon_{\lambda\lambda'}^-)^2 - 4I_{\lambda\lambda'}^2)}{(\varepsilon_{\lambda\lambda'}^+ - \varepsilon_{\lambda\lambda'}^-)^2} (n_F(\varepsilon_{\lambda\lambda'}^-) - n_F(\varepsilon_{\lambda\lambda'}^+)) \\ &\times \delta(\varepsilon_{\lambda\lambda'}^- - \varepsilon_{\lambda\lambda'}^+ + \hbar\omega), \end{aligned} \quad (15.3)$$

here

$$\Phi(\varepsilon_{\lambda\lambda'}^-, \varepsilon_{\lambda\lambda'}^+, r_{\lambda\lambda'}) = \frac{\varepsilon_{\lambda\lambda'}^+ - \varepsilon_{\lambda\lambda'}^-}{\sqrt{(\varepsilon_{\lambda\lambda'}^+ - \varepsilon_{\lambda\lambda'}^-)^2 - 4I_{\lambda\lambda'}^2}}$$

is the Jacobian of the transition from the initial energies $\varepsilon_\lambda^0, \varepsilon_{\lambda'}^0$ (excluding hybridization) to the energies $\varepsilon_{\lambda\lambda'}^-, \varepsilon_{\lambda\lambda'}^+$ corresponding to the wave functions $\psi_{\lambda\lambda'}^-$ and $\psi_{\lambda\lambda'}^+$,

$$\varepsilon_{\lambda\lambda'}^\pm = \frac{\varepsilon_\lambda^0 + \varepsilon_{\lambda'}^0}{2} \pm \frac{1}{2} \sqrt{(\varepsilon_\lambda^0 - \varepsilon_{\lambda'}^0)^2 + 4I_{\lambda\lambda'}^2}, \quad (16)$$

$\Gamma_{\lambda\lambda'} = \varepsilon_{\lambda\lambda'}^+ - \varepsilon_{\lambda\lambda'}^-$. The difference of the average occupation numbers, taking into account the Coulomb interaction between electrons localized simultaneously on a pair of centers λ, λ' , that is present in (15.1)–(15.3) can be represented as [14]

$$\begin{aligned} n_F(\varepsilon_{\lambda\lambda'}^-) - n_F(\varepsilon_{\lambda\lambda'}^+) \\ = \frac{(1 - \exp(-\hbar\omega/kT))}{\exp(-(\varepsilon_{\lambda\lambda'}^+ + e^2/\kappa r_{\lambda\lambda'} - \mu)/kT) + \exp(-\hbar\omega/kT) + 1 + \exp((\varepsilon_{\lambda\lambda'}^- - \mu)/kT)}, \end{aligned} \quad (17)$$

where $\varepsilon_{\lambda\lambda'}^+ = \varepsilon_{\lambda\lambda'}^- + \hbar\omega$, $\varepsilon_{\lambda\lambda'}^- + \varepsilon_{\lambda\lambda'}^+ = \varepsilon_\lambda^0 + \varepsilon_{\lambda'}^0$.

Integration (15.1)–(15.3) under the condition $kT < \hbar\omega$, $e^2/\kappa r_\omega$ ($kT > \hbar\omega$, $e^2/\kappa r_{opt}$) gives for the real part of phononless conductivity (14) in cases of low ($\omega < \omega_{opt}$) and high ($\omega > \omega_{opt}$) frequencies expressions (2) and (4) [13] ((6) and (5) [14]); in this case, we have

$$\begin{aligned} \int_{-\infty}^{\infty} (n_F(\varepsilon_{\lambda\lambda'}^-) - n_F(\varepsilon_{\lambda\lambda'}^- + \hbar\omega)) d\varepsilon_{\lambda\lambda'}^- = \hbar\omega + e^2/\kappa r_{\lambda\lambda'} \\ \text{for } kT < \hbar\omega, e^2/\kappa r_\omega, \end{aligned} \quad (18.1)$$

$$\begin{aligned} \int_{-\infty}^{\infty} (n_F(\varepsilon_{\lambda\lambda'}^-) - n_F(\varepsilon_{\lambda\lambda'}^- + \hbar\omega)) d\varepsilon_{\lambda\lambda'}^- \approx \hbar\omega \\ \text{for } kT > \hbar\omega, e^2/\kappa r_\omega. \end{aligned} \quad (18.2)$$

Let us present the ratios (15.1), (15.2), (15.3), (17) in the following form for calculating the phononless conductivity in the intermediate temperature range

$$\begin{aligned} \sigma_{1a}^{res}(\omega) &= C_0 \sigma_0 \int_{2\ln(\omega_c/\omega)}^{\infty} \frac{x^4 \exp(-x)}{\sqrt{(\omega/\omega_c)^2 - \exp(-x)}} dx \\ &\times \int_{-\infty}^{\infty} (n_F(\varepsilon_{\lambda\lambda'}^-) - n_F(\varepsilon_{\lambda\lambda'}^- + \hbar\omega)) d(\varepsilon_{\lambda\lambda'}^-/\hbar\omega_c), \end{aligned} \quad (19.1)$$

$$\begin{aligned} \sigma_{1b}^{res}(\omega) &= C_0 \sigma_0 \int_{2\ln(\omega_c/\omega)}^{\infty} x^6 \exp(-x) dx \\ &\times \int_{-\infty}^{\infty} (n_F(\varepsilon_{\lambda\lambda'}^-) - n_F(\varepsilon_{\lambda\lambda'}^- + \hbar\omega)) d(\varepsilon_{\lambda\lambda'}^-/\hbar\omega_c), \end{aligned} \quad (19.2)$$

$$\sigma_{1c}^{res}(\omega) = C_2 \sigma_0 \frac{\omega}{\omega_c} \int_{2 \ln(\omega_c/\omega)}^{\infty} x^8 \exp(-x) \sqrt{1 - \frac{\exp(-x)}{(\omega/\omega_c)^2}} dx$$

$$\times \int_{-\infty}^{\infty} (n_F(\varepsilon_{\lambda\lambda'}^-) - n_F(\varepsilon_{\lambda\lambda'}^- + \hbar\omega)) d(\varepsilon_{\lambda\lambda'}^-/\hbar\omega_c) \quad (19.3)$$

where $\sigma_0 = \pi^2 e^4 \rho_0^2 a^4 \omega_c / (3\kappa) = \pi^2 e^2 \rho_0^2 a^5 \hbar \omega_c^2 / 6$, $\omega_c = 2I_0/\hbar$, $I_0 = e^2/\kappa a$, $r_\omega = a \ln(\omega_c/\omega)$, $x = 2r_{\lambda\lambda'}/a$, $C_0 = 1/2^4$, $C_2 = 1/2^6$ — numerical coefficients,

$$n_F(\varepsilon_{\lambda\lambda'}^-) - n_F(\varepsilon_{\lambda\lambda'}^- + \hbar\omega) = \frac{(1 - \exp(-\omega/(\omega_c \vartheta)))}{\exp(-(\tilde{\varepsilon}_{\lambda\lambda'}^- + \omega/\omega_c + 1/x)/\vartheta) + \exp(-\omega/(\omega_c \vartheta)) + 1 + \exp(\tilde{\varepsilon}_{\lambda\lambda'}^-/\vartheta)} \quad (20)$$

$\vartheta = kT/\hbar\omega_c$, $\tilde{\varepsilon}_{\lambda\lambda'}^- = (\varepsilon_{\lambda\lambda'}^- - \mu)/\hbar\omega_c$; in this case, we have

$$\int_{-\infty}^{\infty} (n_F(\varepsilon_{\lambda\lambda'}^-) - n_F(\varepsilon_{\lambda\lambda'}^- + \hbar\omega)) d(\varepsilon_{\lambda\lambda'}^-/\hbar\omega_c) = \omega/\omega_c + 1/x$$

for $kT < \hbar\omega$, $e^2/\kappa r_\omega$ [13], (21.1)

$$\int_{-\infty}^{\infty} (n_F(\varepsilon_{\lambda\lambda'}^-) - n_F(\varepsilon_{\lambda\lambda'}^- + \hbar\omega)) d(\varepsilon_{\lambda\lambda'}^-/\hbar\omega_c) \approx \omega/\omega_c$$

for $kT > \hbar\omega$, $e^2/\kappa r_\omega$ [14]. (21.2)

It should be noted that the energy integration in (15.1)–(15.3) yields $\int_{-\infty}^{\infty} (n_F(\varepsilon_{\lambda\lambda'}^-) - n_F(\varepsilon_{\lambda\lambda'}^- + \hbar\omega)) d\varepsilon_{\lambda\lambda'}^- = \hbar\omega$ without taking into account the Coulomb interaction of electrons falling on isolated pairs of centers (summand $e^2/\kappa r_{\lambda\lambda'}$ in (17)); in this case, the frequency dependence of the real part of the phononless conductivity $\sigma_{1c}^{res}(\omega)$ (14) is independent of temperature and corresponds to the expressions (6) at $\omega < \omega_{opt}$ and (5) at $\omega > \omega_{opt}$, i.e. it agrees with the expressions for $\sigma_{1c}^{res}(\omega)$, obtained taking into account the Coulomb interaction of electrons in pairs at high temperatures $kT > \hbar\omega$, $e^2/\kappa r_{opt}$.

2. Results and conclusions

The results of numerical calculation of the frequency dependences of the real part of phononless conductivity (14) at different temperature values are shown in Figure 1. The results of calculation of $\sigma_{1c}^{res}(\omega, T)$ (14) are consistent, respectively, with the expressions (3), (6) at low frequencies $\omega < \omega_{opt}$ in cases of low ($e^2/\kappa r_\omega$, $\hbar\omega > kT$) and high ($kT > \hbar\omega$, $e^2/\kappa r_{opt}$) temperatures; and they are consistent with the expression $\sigma_{1c}^{res}(\omega)$ (5) at high frequencies $\omega > \omega_{opt}$. An increase of phononless conductivity with a decrease of temperature at a given frequency ($\omega < \omega_{opt}$) is attributable to the main role of the Coulomb interaction between electrons in resonant pairs at low temperatures, $e^2/\kappa r_\omega > \hbar\omega > kT$.

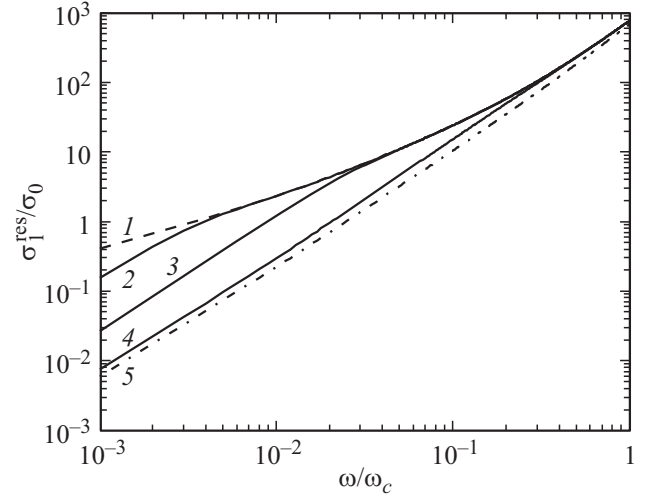


Figure 1. Frequency dependences of the real part of phononless conductivity $\sigma_{1c}^{res}(\omega, T)$ (14) at different temperature values; curve 1 — $T = 0$ K ($e^2/\kappa r_\omega$, $\hbar\omega > kT$), curve 2 — $T = 0.1$ K, curve 3 — $T = 0.7$ K, curve 4 — $T = 8$ K, curve 5 — $kT > \hbar\omega$, $e^2/\kappa r_{opt}$. The curves 1 and 5 at low frequencies $\omega < \omega_{opt}$ correspond to expressions (3) and (6), i.e. $\sigma_{1c}^{res}(\omega)$ in these cases has a sublinear ($s \approx 0.8$) and subquadratic ($s \approx 1.5$) character, respectively; curves 1 and 5 are consistent with the expression (5) ($s \approx 2$) at high frequencies $\omega > \omega_{opt}$.

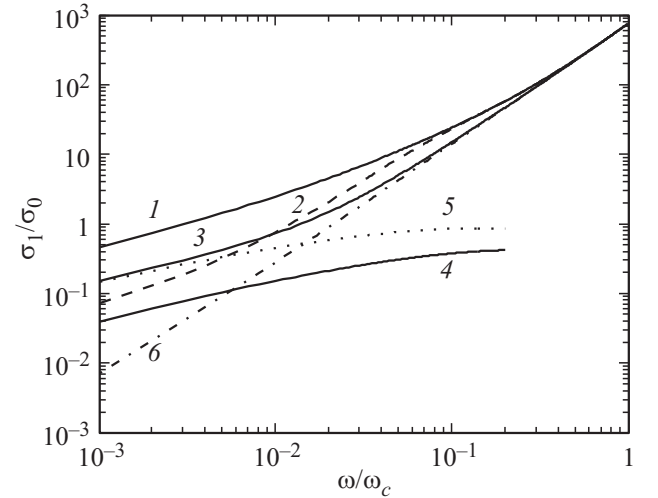


Figure 2. Frequency dependences of the real part of conductivity, $\sigma_1(\omega, T) = \sigma_{1c}^{res}(\omega, T) + \sigma_1^{rel}(\omega, T)$, at different temperature values; curve 1 — $\sigma_1(\omega) \approx \sigma_{1c}^{res}(\omega)$ at $T \approx 0$ K, curve 2 — $\sigma_1(\omega, T)$ at $T = 2.1$ K, curve 3 — $\sigma_1(\omega, T)$ at $T = 10$ K, curve 4 — frequency dependence of relaxation conductivity $\sigma_1^{rel}(\omega, T)$ at $T \approx 0$ K (7), curve 5 — frequency dependence of the interpolation expression for relaxation conductivity $\sigma_1^{rel}(\omega, T)$ (9) at $T = 10$ K, curve 6 — frequency dependence of phononless conductivity $\sigma_{1c}^{res}(\omega, T)$ (14) at $T = 10$ K.

Figure 2 shows the obtained frequency dependences of the real part of the conductivity, taking into account the resonant and relaxation contributions, $\sigma_1(\omega, T) = \sigma_{1c}^{res}(\omega, T) + \sigma_1^{rel}(\omega, T)$, at different temper-

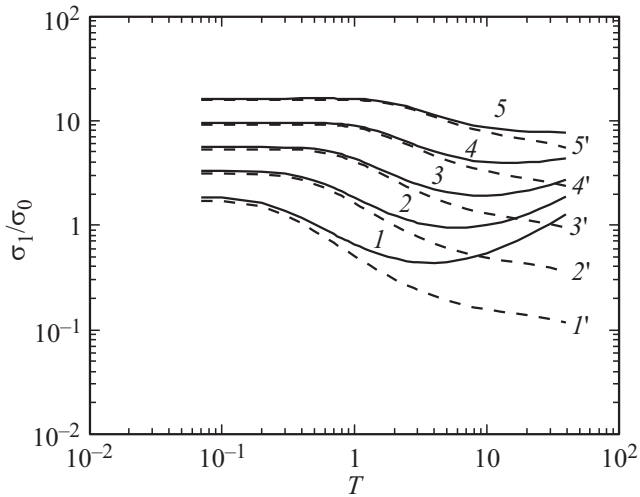


Figure 3. Temperature dependences of high-frequency conductivity, $\sigma_1(\omega, T) = \sigma_1^{res}(\omega, T) + \sigma_1^{rel}(\omega, T)$, at various defined frequency values; curve 1 — $\omega/\omega_c = 0.007$, curve 2 — $\omega/\omega_c = 0.014$, curve 3 — $\omega/\omega_c = 0.025$, curve 4 — $\omega/\omega_c = 0.043$, curve 5 — $\omega/\omega_c = 0.071$. The dashed curve numbers correspond to the temperature dependences of the phononless contribution to conductivity calculated at specified frequency values.

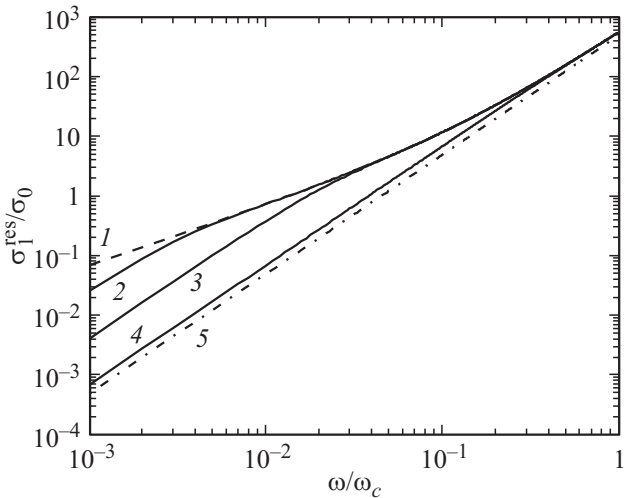


Figure 4. Frequency dependences of the real part of phononless conductivity $\sigma_1^{res}(\omega, T)$ (22) at different temperature values; curve 1 — $T = 0\text{ K}$ ($kT \ll \hbar\omega$, $e^2/\kappa r_{opt}$), curve 2 — $T = 0.1\text{ K}$, curve 3 — $T = 0.7\text{ K}$, curve 4 — $T = 10\text{ K}$, curve 5 — $kT > \hbar\omega$, $e^2/\kappa r_{opt}$. The curves 1 and 5 correspond, respectively, to expressions (4) and (5).

ature values. According to the calculation results, the temperature dependence of high-frequency conductivity with a decrease of temperature reaches saturation in a non-monotonic way due to the multidirectional changes of relaxation and resonance contributions to conductivity with a change of temperature (Figure 3); thus, the contribution from relaxation conductivity decreases with a decrease of temperature at a given frequency, and the contribution

from phononless conductivity increases. The results of the conductivity calculations shown in the figures correspond to the characteristic values of the parameters $\omega_c = 10^{13}\text{ rad/s}$, $\omega_{ph}/\omega_c = 5$.

It should be noted that the sublinearity ($s < 1$) of the frequency dependence of the conductivity of disordered semiconductors, generally speaking, can be determined by the relaxation rather than the resonance component in the transition frequency range at $\omega < \omega_{cr}$. For instance, the hybridization involving states of intermediate centers can misalign the energy levels in resonant pairs with a large center-to-center distance at low frequencies $\omega \ll \omega_c$ corresponding to large values of the optimal hopping distance $r_\omega > N_d^{-1/3}$, in case of the transition of the charge carrier not to the nearest localization center with a close initial energy. Calculation of the real part of phononless conductivity using the basis of localized atomic type functions, $\langle \psi_{\lambda\lambda'}^- | (\mathbf{n}, \mathbf{r}) | \psi_{\lambda\lambda'}^+ \rangle \approx \langle \psi_\lambda | (\mathbf{n}, \mathbf{r}) | \psi_{\lambda'} \rangle$,

$$\sigma_1^{res}(\omega) = \pi e^2 \omega \rho_0^2 \iiint d\varepsilon_\lambda d\varepsilon_{\lambda'} d\mathbf{r}_{\lambda\lambda'} |\langle \psi_\lambda | (\mathbf{n}, \mathbf{r}) | \psi_{\lambda'} \rangle|^2 \times (n_F(\varepsilon_\lambda) - n_F(\varepsilon_{\lambda'})) \delta(\varepsilon_\lambda - \varepsilon_{\lambda'} + \hbar\omega), \quad (22)$$

$$\sigma_1^{res}(\omega) = C_2 \sigma_0 \frac{\omega}{\omega_c} \int_0^\infty x^8 \exp(-x) dx \times \int_{-\infty}^\infty (n_F(\varepsilon_\lambda) - n_F(\varepsilon_\lambda + \hbar\omega)) d(\varepsilon_\lambda/\hbar\omega_c), \quad (23)$$

yields the expression (4) in the low temperature range, $kT \ll \hbar\omega$, $e^2/\kappa r_{opt}$, and it yields the expression (5) in the conditions, $kT > \hbar\omega$, $e^2/\kappa r_{opt}$; the frequency dependences of the real part of phononless conductivity $\sigma_1^{res}(\omega)$ (22) over the entire temperature range studied are superlinear ($s > 1$) (Figure 4). The calculation of phononless conductivity using the basis of atomic-type functions (in the mode with a constant hopping distance) gives a lower value of conductivity in the frequency range $\omega < \omega_{cr} \sim \omega_{opt}$ compared to the result of calculation of phononless conductivity using the basis of pairwise hybridized wave functions (in the mode with a variable hopping distance); at the same time the sublinearity of the frequency dependence of the conductivity of disordered semiconductors in the frequency range $\omega < \omega_{cr}$ is determined by the predominant relaxation component (Figure 5). The non-monotonicity of the temperature dependence of the real part of the conductivity is smoothed out in the frequency range $\omega \ll \omega_{cr}$ according to the performed calculations; at the same time, the non-monotonicity albeit less pronounced in the behavior of $\sigma_1(\omega, T)$ is still present for frequencies corresponding to the transition region (Figure 6). The non-monotonicity of the temperature dependence of conductivity $\sigma_1(\omega, T)$ in the low temperature region is attributable to the multidirectional changes in relaxation and resonance contributions to conductivity with temperature changes, the predominance of phononless contributions, and the main role of the

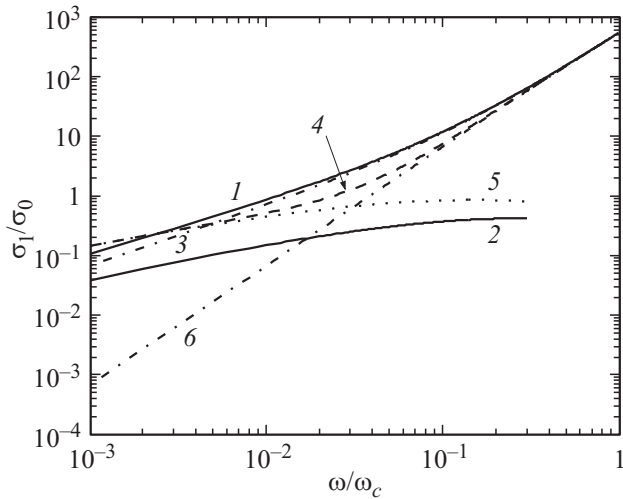


Figure 5. Frequency dependences of the real part of the conductivity at different temperature values; curve 1 — $\sigma_1(\omega, T) = \sigma_1^{res}(\omega, T) + \sigma_1^{rel}(\omega, T)$ at $T \approx 0$ K, curve 2 — frequency dependence relaxation conductivity $\sigma_1^{rel}(\omega)$ (7), curve 3 — frequency dependence of phononless conductivity $\sigma_1^{res}(\omega, T)$ (22) at $T \approx 0$ K, curve 4 — $\sigma_1(\omega, T)$ at $T \approx 10$ K, curve 5 — frequency dependence of the interpolation expression for relaxation conductivity (9) at $T = 10$ K, curve 6 — frequency dependence of phononless conductivity $\sigma_1^{res}(\omega, T)$ (22) at $T = 10$ K.

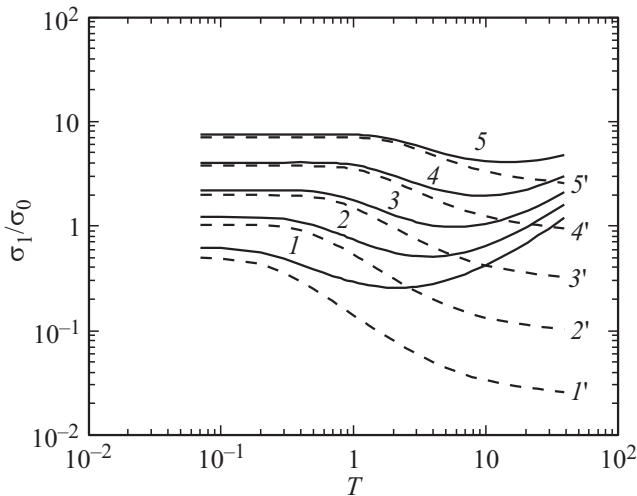


Figure 6. Temperature dependences of high-frequency conductivity, $\sigma_1(\omega, T) = \sigma_1^{res}(\omega, T) + \sigma_1^{rel}(\omega, T)$, at various defined frequency values; curve 1 — $\omega/\omega_c = 0.007$, curve 2 — $\omega/\omega_c = 0.014$, curve 3 — $\omega/\omega_c = 0.025$, curve 4 — $\omega/\omega_c = 0.043$, curve 5 — $\omega/\omega_c = 0.071$. The shaded curve numbers correspond to the temperature dependences of the phononless contribution to conductivity (22), calculated at specified frequency values.

Coulomb interaction between electrons in pairs contributing to phononless conductivity in the low temperature region, $e^2/\kappa r_{opt} > \hbar\omega > kT$.

A superlinearity ($s > 1$) of the frequency dependence of the real part of low-temperature conductivity $\sigma_1(\omega)$ was

found in some experiments on Si:P [9] in the frequency range of 100–500 GHz, which was associated with a manifestation of the Coulomb gap in a single-particle density of states describing the distribution of self-consistent energies ε_i of interacting localized charge carriers in the ground state of the system. We would like to remind that the soft Coulomb gap in a single-particle density of states $\rho(\varepsilon)$ in the vicinity of the Fermi level is determined by the stability of the ground state of the system relative to single-electron transitions. However, the spectrum of excitations created by photon absorption at low temperatures is not directly related to the single-particle density of states $\rho(\varepsilon)$, which describes the distribution of self-consistent energies corresponding to the addition of an electron to the ground state of the system. The energy of the final state φ_f during the transition corresponds to the addition of an electron to a state that differs from the ground state in that the center i is empty (occupied by a hole); in this case, we have $\varphi_f = \varepsilon_f - e^2/\kappa r_{if}$, $\varphi_i = \varepsilon_i$, where r_{if} is the center-to-center distance.

The calculation of low-temperature phononless conductivity in Ref. [16] using the concept of self-consistent energies showed that the frequency dependence of phononless conductivity has the form (4), i.e. it is consistent with the results of calculating the frequency dependence of low-temperature phononless conductivity at high frequencies, when the effects of hybridization are insignificant and the optimal hopping distance r_{opt} does not depend on the frequency [13]. The optimal hopping distance r_{opt} corresponds to transitions outside the Coulomb gap. Extrapolation of the results of the standard approach from the region of almost linear frequency dependence of conductivity with variable hopping distance to the region of quadratic frequency dependence of conductivity with constant hopping distance corresponds to a sublinear frequency dependence of conductivity in the low frequency region ($s \approx 0.8$ at $\omega \ll \omega_{cr}$). Thus, the superlinearity of the frequency dependence of the conductivity $\sigma_1(\omega)$ in the transition frequency range may be due to the transition from a variable to a constant (independent of frequency) optimal hopping distance r_{opt} .

Based on the above, we would like to note that data on its temperature dependence in the low temperature region are essential to establish the characteristics of the effect of Coulomb effects on the low-temperature high-frequency conductivity of disordered semiconductors.

Conflict of interest

The authors declare that they have no conflict of interest.

References

- [1] N.A. Poklonski, S.A. Vyrko, A.G. Zabrodskii. FTT **47**, 7, 1195 (2005). (in Russian).
- [2] N.F. Mott. Phil. Mag. **22**, 7 (1970).
- [3] B.I. Shklovskii, A.L. Efros. JETP **54**, 1, 218 (1981).
- [4] I.G. Austin, N.F. Mott. Adv. Phys. **18**, 71, 41 (1969).

- [5] A.L. Efros. *Phil. Mag. B* **43**, 5, 829 (1981).
- [6] A.L. Efros, B.I. Shklovskii. In: *Electron-Electron Interactions in Disordered Systems* / Eds A.L. Efros, M. Pollak. North Holland, Elsevier Science Publishers B.V., Amsterdam (1985). P. 409.
- [7] I.P. Zvyagin. In: *Charge Transport in Disordered Solids with Applications in Electronics* / Ed. S. Baranovski. John Wiley & Sons, Chichester (2006). Ch. 9. P. 339.
- [8] E. Helgren, N.P. Armitage, G. Grüner. *Phys. Rev. B* **69**, 014201 (2004). E. Helgren, N.P. Armitage, G. Grüner. *Phys. Rev. Lett.* **89**, 246601 (2002).
- [9] M. Hering, M. Scheffler, M. Dressel, H.V. Lohneysen. *Phys. Rev. B* **75**, 205203 (2007).
- [10] E. Ritz, M. Dressel. *Phys. Stat. Sol. (c)*, **5**, 703 (2008).
- [11] M. Lee, M.L. Stutzmann. *Phys. Rev. Lett.* **87**, 056402 (2001).
- [12] I.P. Zvyagin, M.A. Ormont. *Moscow Univ. Phys. Bull.* **63**, 4, 272 (2008).
- [13] M.A. Ormont, I.P. Zvyagin. *Semicond.* **54**, 1, 33 (2020).
- [14] M.A. Ormont, N.V. Valenko. *Phys. Solid State* **65**, 7, 1192 (2023).
- [15] V.L. Bonch-Bruевич, I.P. Zvyagin, R. Kaiper, A.G. Mironov, R. Enderlain, B.-M. Esser. *Elektronnaya teoriya neuporyadochennykh poluprovodnikov*. Nauka, M. (1981). (in Russian).
- [16] M.A. Ormont. *Moscow Univ. Phys. Bull.* **66**, 2, 162 (2011).

Translated by A.Akhtyamov